Exploring the Degree of Relative Crystalline and Amorphous Properties of Cellulose Nanofibers by Correlated Graphene-Quenching Raman Spectroscopy with Electrostatic Force Microscopy Technique

Won-Hwa Park (s952151@gmail.com)
Inha University

Research Article

Keywords: Degree of Relative Crystalline and Amorphous Properties, Individual cellulose nanofiber, Graphene-Quenching Raman Spectroscopy, Electrostatic Force Microscopy

Posted Date: March 24th, 2022

DOI: https://doi.org/10.21203/rs.3.rs-1448404/v1

Exploring the Degree of Relative Crystalline and Amorphous Properties of Cellulose Nanofibers by Correlated Graphene-Quenching Raman Spectroscopy with Electrostatic Force Microscopy Technique

Won-Hwa Park *

Department of Chemical Engineering, Inha University, 100 Inha-ro, Michuhol-gu, Incheon, 22212, Republic of Korea, E-mail: s952151@gmail.com

Utilizing cellulose nanofibers (CNF) attracts tremendous attention in terms of developing a non-breakable film with high toughness and optically transparent properties. Here, the author introduces a new characterization method in order to compare the relative degree of the crystalline and amorphous characters of CNF by correlating Graphene-Quenching Raman Scattering (GQRS) with Electrostatic Force Microscope (EFM) results. This nano-metrology may pave the new way in quantitatively unraveling the degree of lignin and hemicellulose.

KEYWORD: Degree of Relative Crystalline and Amorphous Properties, Individual cellulose nanofiber, Graphene-Quenching Raman Spectroscopy, Electrostatic Force Microscopy

From a few decades ago, cellulose materials frequently offer the normal standard to determine the degree of eco-compatibility and this property makes cellulose materials for a variety of fields as eco-friendly functional materials not to harm the surrounding environment [1]. Moreover, cellulose is one of the naturally abundant materials and can be produced and exfoliated as a nanofiber type formation by chemical and mechanical pre-treatment from woods, plants, bacteria, and tunicate [2]. Especially, cellulose nanocrystal (CNC) division has a pivotal role in showing strong mechanical, transparent, and flexible properties [3]. One of the main applications with its unique properties in CNC can be fitted into employed in the fabrication of macro-and nano-dimensional film with high optical transparency and toughness [4, 5].

Herein, the author attempts to develop a new characterization nano-metrology that can unveil the superior factor in terms of making a highly transparent and tough film.

Each cellulose sample from raw biomass materials is primarily solvated into deionized (DI) water and mixed with phosphoric groups ($H_2PO_4^-$) to enhance electrostatic repulsive force between CNF to chemically fabricate individual CNF. After that, the hydrolysis process using strong sulfuric acid is employed in order to make non-aggregate and well-dispersed CNC [6]. The heating and mechanical grinding by homogenizer are sequentially applied [7]. From these procedures, the author can anticipate the further formation of the individualized CNCs, as defined medium-density fibreboard (MDF) and medium-density fibreboard (HDF) between softwood and hardwood cellulose in this experiment.

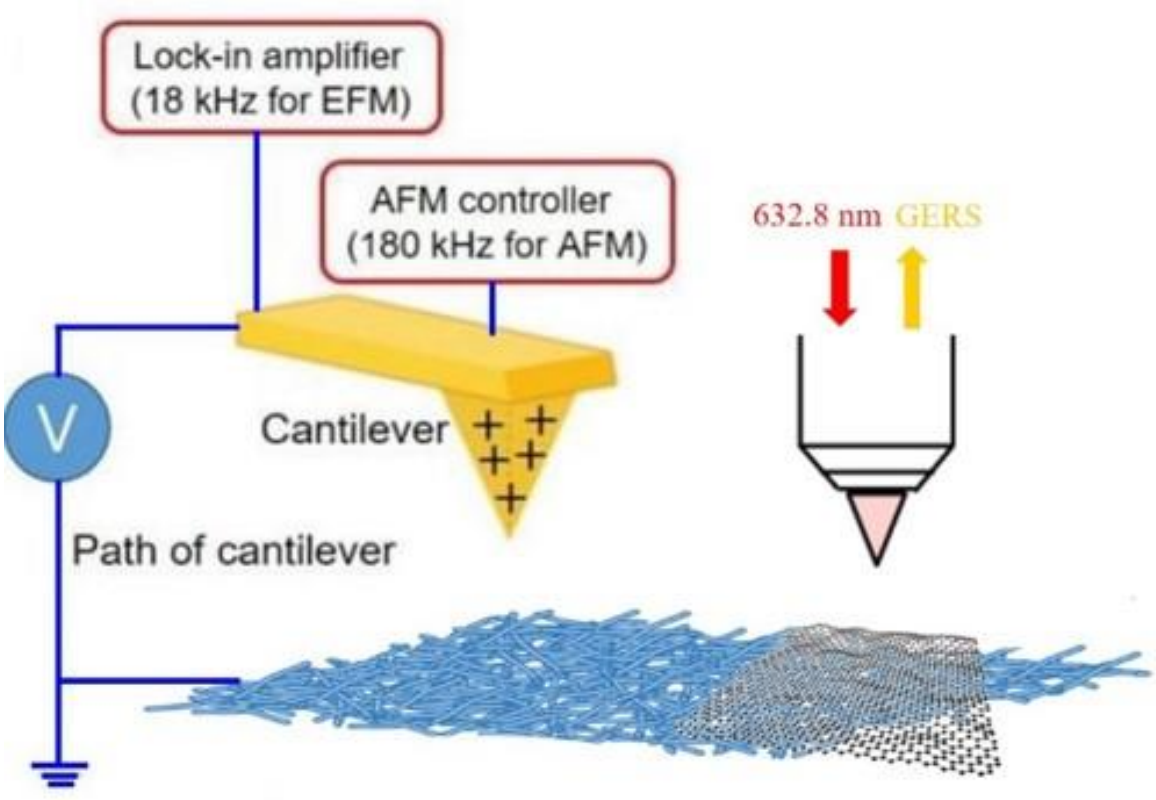

Scheme. 1 Schematic picture showing an experimental apparatus in this work. Briefly, the principle of Electrostatic Force Microscope (EFM) image acquisition can be illustrated in the left part, in which the nanoscale electrostatic interaction between sample and tip under a certain bias is employed during scanning [8, 9]. Separately, the confocal Raman spectrum using CNF can be obtained by 632.8 nm excitation with CVD-grown graphene monolayer (CVD-GM) on SiO_2/Si substrate so as to efficiently eliminate the unwanted fluorescence background signal by virtue of the quenching effect from the underneath CVD-GM substrate.

Scheme 1 exhibits the illustration of experimental apparatus for doing both EFM and Graphene-Quenching Raman Scattering (GQRS) characterizations. Briefly, EFM maps the electrical properties of a sample surface by measuring the electrostatic force between the surface and a biased Au-coated Atomic Force Microscope (AFM) cantilever. EFM, a voltage is applied between the tip and the sample (tip = 5 V and sample = 0 V) while the cantilever hovers above the surface, not touching it. The cantilever deflects when it scans over a static charge. To obtain an EFM image it is necessary to separate the overall EFM signal into a topographic AFM image and an EFM image at the same time and at the same location. The key issue to resolving it is to apply the single-pass technique. In short, the tip is scanned over the surface while oscillating at a frequency f (here ~180 kHz), obtaining a non-contact AFM image of the surface topography. At the same time, the author employs an AC bias to the tip at the frequency ω (here ~18 kHz) through an external lock-in amplifier and also applies a DC bias from the control

electronics. Therefore, the author can disentangle the topographic image and the EFM image simultaneously [8, 9]. The GQRS spectra can be obtained using a high numerical aperture (N.A. 0.9) air-immersion objective lens with 632.8 nm excitation. In particular, the gel-type cellulose samples are loaded onto the CVD-GM/SiO_2/Si substrate to efficiently remove the unwanted luminescence such as auto-fluorescence from the samples [10, 11]

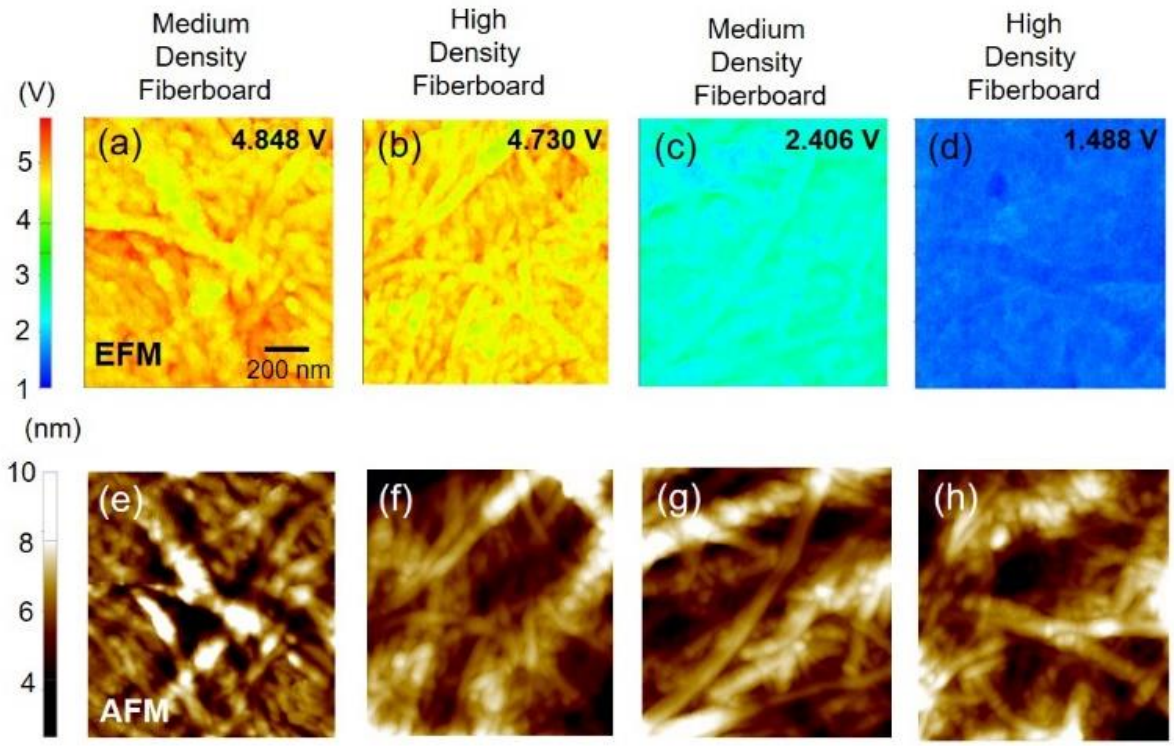

Fig. 1 (a) ~ (d) shows the electrostatic force microscope (EFM) images between hardwood of (a)/(b) and softwood CNF of (c)/(d) with different degrees of density, confirmed by the corresponded AFM images of (e) ~ (h), with the above EFM images. The EFM amplitude voltage of the hardwood set of (a)/(b) exhibits a relatively higher voltage value than the softwood case. The higher density of each wood CNF also shows the lower EFM voltage value.

Figure 1 shows the EFM and AFM images of CNF, corresponding between the above and below, respectively, such as (a) and (e). The author can also distinguish between (a)/(b) and (c)/(d) as hardwood (bamboo) and softwood (needle leaf tree) CNF, respectively. In both hardwood and softwood, the author can further disentangle MDF and HDF by the different degrees of mechanical grinding and homogenizer treatment. Preferentially, the author can investigate the different averaged EFM amplitude voltage between Figure 1(a) and (b). At this time, it is worthwhile to note that the higher EFM voltage means the Au-coated tapping amplitude is relatively larger due to less electrostatic attractive force between the tip and sample, indicating this sample is a more hydrophobic, larger

population of CNC, and reflects less distribution of lignin and hemicellulose accordingly [12-14]. Moreover, it can be also deduced that the reason for the higher EFM voltage (4.848 V) image in Figure 1(a) than 1(b) may be attributable to the degree of entanglement of CNF formation, in which the MDF of Figure 1(a) is clearly visible as separate CNCs with the lower aspect ratio shape from the corresponding AFM image in Figure 1(e), following the near-individual formation [15, 16], whereas the HDF sample in Figure 1(b) with relatively lower EFM voltage (4.730 V) is shown likewise relatively higher entanglement and somewhat higher aspect ratio rather than the MDF according to the corresponding AFM image in Figure 1(f), resulting in strong intra- and intermolecular hydrogen bond interaction and strong affinity [17]. Therefore, the hydrophilic properties originated from the relatively higher amount of lignin and hemicellulose may be anticipated in Figure 1(b) with the smaller population of CNC, and reflects more distribution of lignin and hemicellulose accordingly.

In this regard, the author can also acknowledge in Figure 1(c)/(g) and 1(d)/(h) as the analogous case to the hardwood results except for the different origins of CNF (Softwood). In general, the composition of hardwood (bamboo) was determined to be 40~46% cellulose, 17~23% hemicelluloses, 18~25% lignin while the composition of softwood (needle leaf tree) was known to be 45~50% cellulose, 19~22% hemicelluloses, 21~29% lignin [18]. From this report, the significantly lower EFM voltage in softwood cases can be ascribed to the higher population of lignin components. According to the chemical structure of lignin, a lot of conjugated π-electrons and hydroxyl groups are present and may have a role to exhibit relatively hydrophilic properties, especially, in amorphous or disordered domains in CNF [19]. As such, it can be interpreted that a higher concentration of lignin in softwood shows significantly lower EFM voltage in this experiment. Moreover, the degree of mechanical treatment by grinding and homogenizer also influences the slightly different EFM voltage (0.918 V) between Figure 1(c) and 1(d) by exploring the corresponding Figure 1(g)/(h) AFM images, respectively, likewise Figure 1(e)/(f) in hardwood case.

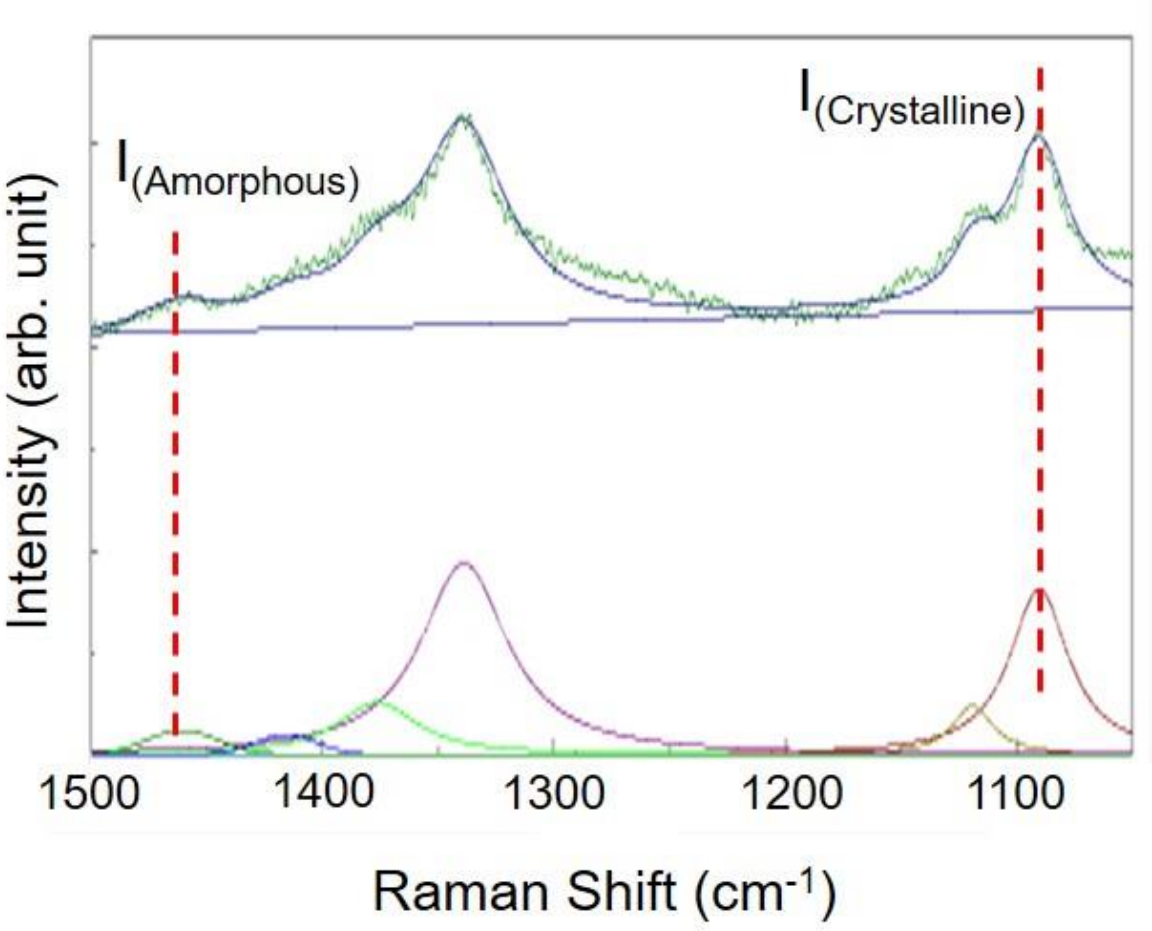

Fig. 2 The representative GQRS spectrum of CNF sample in this experiment with the assignment of two peak modes at ~1482 cm^{-1} and ~1090 cm^{-1} as $I_{(Amorphous)}$ and $I_{(Crystalline)}$, respectively, [20, 21].

According to the reference [20, 21], the author can assign two significant peak modes. At ~1090 cm^{-1} is the COC stretching symmetric vibrational mode, meaning that the existence of the crystalline chemical structure (or skeletal backbone structure) of CNC can be evidenced. Hence, the author can regard the COC stretching symmetric vibrational mode as $I_{(Crystalline)}$. In contrast, the peak at ~ 1482 cm^{-1} is assigned as HCH scissoring bending mode and can be utilized as $I_{(Amorphous)}$ in this work.

Furthermore, the author tries to obtain the correlated results with the aforementioned data by GQRS spectroscopy. Graphene is well-known thin-film material, especially, whose has a role to quench the unwanted luminescence or auto-fluorescence from nearby organic molecules to evidently investigate the Raman peaks without background signal on the basis of linear non-radiative energy transfer of organic molecules to near Dirac points of graphene [10, 11]. Figure 2 shows a representative background-free GQRS spectrum (up) and the subsequent de-convoluted (bottom), as shown in the right part of scheme 1. According to the previous reports, the author can assign the two representatives Raman peaks. At ~1090 cm^{-1} was assigned as COC stretching symmetric

vibrational mode, displaying the crystalline chemical structure (or skeletal backbone structure) of CNF and applied as $I_{(Crystalline)}$, whereas, the peak at ~ 1482 cm^{-1} is assigned as HCH scissoring bending mode and can be utilized as $I_{(Amorphous)}$ in this work [20]. In order to compare the degree of amount of lignin (or hemicellulose), the author can acquire the $I_{[Amorphous]}$/ $I_{(Crystalline)}$ value from the de-convoluted GQRS spectrum quantitative evaluation.

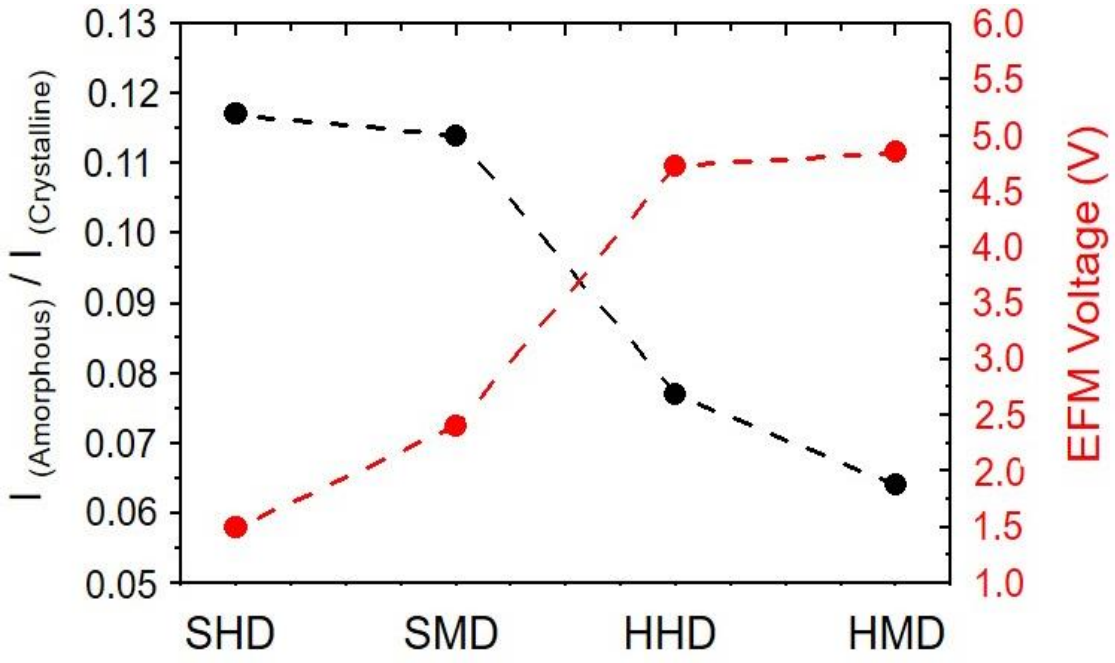

Fig. 3 In order to compare the degree of the relative amount of lignin or (hemicellulose) in each wood cellulose, the author employs the $I_{(Amorphous)}/I_{(Crystalline)}$ value in the left axis and the corresponded overall EFM voltage acquired from the EFM images in the right axis as a function of both wood types and the degree of mechanical treatment. Consequently, the author can unveil the anti-correlation in that the highest degree of amorphous CNF from GQRS fits into the lowest EFM voltage in the SHD sample. Note that the SHD is softwood high density, SMD is softwood medium density, HHD is hardwood high density, and HMD is hardwood medium density.

In Figure 3, the author can plot between the I(Amorphous)/I(Crystalline) value from the GQRS spectrum obtained in Figure 2 and the EFM voltage obtained in Figure 1 in the right axis as a function of a different kind of wood (soft/hard) and mechanical treatment of CNFs. Interestingly, the author can find out the anti-correlation plot, meaning that the CNF with the highest EFM voltage (HMD) is in sync with the lowest $I_{(Amorphous)}/I_{(Crystalline)}$ value. It indicates that the degree of the highest hydrophobic property is clearly correlated to the degree of the highest crystalline in the HMD sample in this experiment. Therefore, the hardwood with medium density (HMD) CNF can be claimed as the most useful CNF in terms of achieving high transparency with high toughness considering

the minimum amount of lignin (or hemicellulose), which is in good agreement with the author's belief. In contrast, the lowest EFM voltage CNF is correlated to the highest $I_{(Amorphous)}/I_{(Crystalline)}$ value, which is understood from a maximum amount of lignin (or hemicellulose) in the case of SHD-CNF.

To summarize, the author suggests and introduces a new nano-metrology tool in order to quantitively evaluate the degree of amount of lignin (or hemicellulose) in wood-type cellulose nanofiber. By trying to obtain both EFM voltage and $I_{(Amorphous)}/I_{(Crystalline)}$ value from the GQRS spectrum at the same CNF samples, the author can specifically show the anti-correlation result between them and utilize it to assess what kinds of factors are important to fabricating a film with high toughness and transparent properties, which is deservedly preferable with the highest EFM voltage, as well as the lowest $I_{(Amorphous)}/I_{(Crystalline)}$ value. With these characterizations and subsequent data analysis, the author expects it as one of the most useful methods to support and develop the new CNF-related materials.

Acknowledgement / Funding

This research was funded by the Basic Science Research Program through the National Research Foundation of Korea (NRF) funded by the Ministry of Education (2021R1I1A1A01058271).

Authors' contributions

The author carried out all tasks associated with the elaboration of the manuscript: conception, design, result analysis, and writing.

Availability of data and material

The datasets generated during and/or analyzed during the current study are available from the corresponding author on reasonable request.

Code availability (software application or custom code)

The datasets generated during and/or analyzed during the current study are available from the corresponding author on reasonable request.

Declarations

Conflicts of Interests

The author declares no conflict of interest.

Consent to Participate

Not applicable

Consent of Publication

Not applicable

Ethics approval

Not applicable

Received: ((will be filled in by the editorial staff))
Revised: ((will be filled in by the editorial staff))
Published online: ((will be filled in by the editorial staff))

References

1. Habibi Y, Lucia LA, Rojas OJ (2010) Cellulose Nanocrystals: Chemistry, Self-Assembly, and Applications. *Chem. Rev.,* 110: 3479-3500
2. Moon RJ, Martini A, Nairn J, Simonsen J, Youngblood J (2011) Cellulose nanomaterials review: structure, properties and nanocomposites. *Chem. Soc. Rev.,* 40: 3941-3994
3. Zhao Y, Moser C, Lindstrom ME, Henriksson G, Li J (2017) Cellulose Nanofibers from Softwood, Hardwood, and Tunicate: Preparation–Structure–Film Performance Interrelation. *ACS Appl. Mater. Interfaces.,* 9: 13508-13519
4. Henriksson M, Berglund LA, Isaksson P, Lindstrom T, Nishino T (2008) Cellulose Nanopaper Structures of High Toughness. *Biomacromolecules,* 9: 1579–1585
5. Zhao M, Ansari F, Takeuchi M, Shimizu M, Saito T, Berglund LA, Isogai A (2018) Nematic structuring of transparent and multifunctional nanocellulose papers. *Nanoscale Horiz.* 3: 28-34
6. Habibi Y, Goffin AL, Schiltz N, Duquesne E, Dubois P, Dufresne A (2009) Bionanocomposites based on poly(ε-caprolactone)-grafted cellulose nanocrystals by ring-opening polymerization. *J. Mater. Chem.,* 18: 5002-5010
7. Messa LL, Faez R, Hsieh YL (2021) Phosphorylated cellulose nanofibriles from sugarcane bagasse with pH tunable gelation. *Carbohydrate Polymer Technologies and Applications*, 2: 100085
8. Park WH, Park SG, Kang M, Hyun MS, Choi N, Kim DH, Choo J (2019) Direct visualization of a surface-enhanced Raman spectroscopy nano-gap via electrostatic force microscopy: Dependence on charge transfer from the underlying surface nano-gap distance. *Appl. Surf. Sci.,* 479: 874-878
9. Park WH, Noh SH, Joo MH, Kim TH, Park W, Jung M, Park KH (2013) Characterization of local charge distribution of polyethylene terephthalate film and influence as a graphene substrate. *Appl. Phys. Lett.*, 103: 033107
10. Xie L, Ling X, Fang Y, Zhang H, Liu Z (2009) Graphene as a Substrate To Suppress Fluorescence in Resonance Raman Spectroscopy. *J. Am. Chem. Soc*., 131: 9890–9891
11. Huang J, Lu J, Zhang Y, Xie S, Lin G, Lin W, Zhuang P, Z Zhu, Guo S, Zhang S, Ge Q, Zhang X, Cai W (2021) Vertically Oriented Graphene for the Fluorescence Quenching Raman Spectra of Aromatic Dyes. *J. Phys. Chem. C.*, 125: 14891–14896
12. Dong XM, Kimura T, Revol JF, Gray DG (1996) Effects of Ionic Strength on the Isotropic−Chiral Nematic Phase Transition of Suspensions of Cellulose Crystallites. *Langmuir*, 12: 2076–2082

13. Rojas OJ, Montero GA, Habibi Y (2009) Electrospun nanocomposites from polystyrene loaded with cellulose nanowhiskers. *J. Appl. Polym. Sci.,* 113: 927-935
14. Bai W, Holbery J, Li K (2009) A technique for production of nanocrystalline cellulose with a narrow size distribution. *Cellulose*, 16: 455–465
15. Wu Q, Li X, Li Q, Wang S, Luo Y (2019) Estimation of Aspect Ratio of Cellulose Nanocrystals by Viscosity Measurement: Influence of Aspect Ratio Distribution and Ionic Strength. *Polymers*, 11: 781
16. Parker RM, Guidetti G, Williams CA, Zhao T, Narkevicius A, Vignolini S, Frka-Petesic B (2018) *Adv. Mater.,* The Self-Assembly of Cellulose Nanocrystals: Hierarchical Design of Visual Appearance. 30: 1704477
17. Lindman B, Medronho B, Alves L, Costa C, Edlund H, Norgrena M (2017) The relevance of structural features of cellulose and its interactions to dissolution, regeneration, gelation and plasticization phenomena. *Phys. Chem. Chem. Phys.*, 19: 23704—23718
18. Schutyser W, Renders T, Bossche GVd, Bosch, SVd, Koelewijn SF, Ennaert T, Sels BF (2017) *Catalysis in Lignocellulosic Biorefineries: The Case of Lignin Conversion*, Wiley
19. Khodayari A, Thielemans W, Hirn U, Van Vuure AW, Seveno D (2021) Cellulose-hemicellulose interactions - A nanoscale view. *Carbohydr. Polym*., 270: 118364
20. Szymańska-Chargot M, Cybulsk J, Zdunek A (2011) Sensing the Structural Differences in Cellulose from Apple and Bacterial Cell Wall Materials by Raman and FT-IR Spectroscopy. *Sensors*, 11: 5543-5560
21. Schenzel K, Fischer S (2001) Schenzel K, Fischer S (2001) NIR FT Raman Spectroscopy–a Rapid Analytical Tool for Detecting the Transformation of Cellulose Polymorphs. *Cellulose*, 8: 49–57